Biocatalysis and Agricultural Biotechnology 19 (2019) 101154

Contents lists available at ScienceDirect

Biocatalysis and Agricultural Biotechnology

journal homepage: www.elsevier.com/locate/bab

Biogenic synthesis and characterization of cobalt oxide nanoparticles for catalytic reduction of direct yellow-142 and methyl orange dyes

Tahir Rasheed[a], Faran Nabeel[a], Muhammad Bilal[b,*], Hafiz M.N. Iqbal[c,**]

[a] School of Chemistry & Chemical Engineering, State Key Laboratory of Metal Matrix Composites, Shanghai Jiao Tong University, Shanghai, 200240, China
[b] School of Life Science and Food Engineering, Huaiyin Institute of Technology, Huaian, 223003, China
[c] Tecnologico de Monterrey, School of Engineering and Sciences, Campus Monterrey, Ave. Eugenio Garza Sada 2501, Monterrey, N.L., CP 64849, Mexico

ARTICLE INFO

Keywords:
Bio-catalysis
Cobalt oxide nanoparticles
Taraxacum officinale
Bio-degradation
Synthetic dyes

ABSTRACT

The synthesis of cobalt oxide nanoparticles (CoNPs) using plant extracts is convenient, cheap, eco-friendly, less energy-intensive, and eliminate the use of toxic materials. Naturally occurring phytoconstituents such as flavonoids and phenolics in the *Taraxacum officinale* (*T. officinale*) plant extract can act as capping and stabilizing agents during CoNPs formation process. This study presents the biogenic synthesis of CoNPs using *T. officinale* plant extract using sodium borohydride ($NaBH_4$) as a reducing agent. As developed *T. officinale* CoNPs were designated as TO-CoNPs and initially characterized using various instrumental techniques including UV–Vis spectroscopy, Fourier transform infrared spectroscopy (FT-IR), scanning electron microscopy (SEM), and transmission electron microscopy (TEM). A broad peak at 319 nm region confirms the successful synthesis of TO-CoNPs. The optimally yielded TO-CoNPs were then employed to test their dye degradation potential against azo dyes, i.e., direct yellow-142 and methyl orange. The time-dependent degradation process was performed for 60 min, and sampling was done with each 15 min interval. As compared to the control sample (trialed in the absence of TO-CoNPs), both test sample (trialed in the presence of TO-CoNPs) showed complete degradation of direct yellow-142 and methyl orange dyes at the end of 60 min treatment cycle. In conclusion, the degradation of both azo dyes suggests that TO-CoNPs may also be exploited against other related and emerging contaminants in an eco-benign and cost-effective manner.

1. Introduction

Aiming to protect and rescue environmental and living ecosystem, sustainability agenda from green chemistry has gained special research interests. In past, numerous industrial practices such as heavy consumption of synthetic dyes (one of the major class of synthetic organic compounds) in different industrial sectors, e.g., textile, leather, paper, plastic, food, cosmeceutical and pharmaceutical has posed serious environmental and health hazards (Bilal et al., 2018a, 2019a; Fathima et al., 2018). Also, their controlled or uncontrolled release into the main water bodies with or without partial and inefficient treatments results in significant environmental pollution (Bilal et al., 2017a). Undoubtedly, the industrial sector is a paramount driving force for the economic and technological development of society. Despite that and as discussed above, the growing industrialization impact on widespread environmental concerns due to increased discharge of wastes loaded with baleful, hazardous, and carcinogenic contaminants such as dyes and other hazardous pollutants (Kusic et al., 2006; Bilal et al., 2019b; Liu et al., 2019; Rasheed et al., 2019). Among top priority environmental pollutants, industrial synthetic dyes and dye-based wastewater effluents, endocrine disrupters, pesticides, phenols, and halogenated phenols, polycyclic aromatic hydrocarbons, polychlorinated biphenyls, and other xenobiotics are of supreme concern (Bilal et al., 2018a, 2018b). Therefore, effective degradation or removal of above-coated hazardous contaminants have emerged as a major concern for biotechnologists and environmental scientists. So far, various remediation strategies such as chemical, physiochemical, and biological treatments have been proposed. However, each one has its own merits and demerits over others.

Among chemical, physiochemical, and biological methods for hazardous dye degradation, nanoparticles (NPs)-based reductive degradation has considerable features such as facile in the process, high catalytic efficacy, fast and low-cost, in nature (Fathima et al., 2017). Moreover, NPs-based dye degradation/removal is easy to implement at

---

* Corresponding author.
** Corresponding author.
E-mail addresses: bilaluaf@hotmail.com (M. Bilal), hafiz.iqbal@tec.mx (H.M.N. Iqbal).

https://doi.org/10.1016/j.bcab.2019.101154
Received 29 March 2019; Received in revised form 5 May 2019; Accepted 8 May 2019

Table 1
Physiochemical characteristics of synthetic textile dyes used in this study.

Dye name	CAS ID	Color	λ_{max} (nm)	MW (g/mol)	Molecular formula	Structure
Methyl orange	547-58-0	Orange	464	327.33	$C_{14}H_{14}N_3NaO_3S$	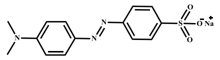
Direct yellow-142	71902-08-4	Yellow	410	794.73	$C_{31}H_{28}N_{10}Na_2O_9S_2$	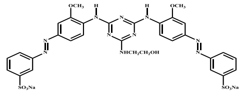

the industrial level. So far, a wide array of NPs regardless of source and type, e.g., zero-valent iron (Fe^o), iron-based bimetallic nanoparticle, biogenic silver, and gold-based NPs, cobalt-based NPs and/or the combination of two such as iron-nickel bimetallic NPs have been used for reductive dye degradation (Bokare et al., 2008; Sha et al., 2016; Rasheed et al., 2018; Vasantharaj et al., 2019a,b). Among all, cobalt-based NPs have gained high research interests and emerged as a promising catalytic agent to treat azo dyes via catalytic reduction degradation route (Naz et al., 2014). Additionally, cobalt-based NPs exhibit high resistance to oxidation, corrosion, and wear (Naz et al., 2014).

As discussed earlier, the green chemistry agenda insists on avoiding or at least reducing the environmental and human-health related problems of toxic chemicals and solvents. In this context, biogenic NPs prepared via green chemistry route are process-friendlier and environmentally benevolent. In an earlier study, Rasheed et al. (2018) reported green biosynthesis of silver-based NPs with promising catalytic potentialities. *Taraxacum officinale* (*T. officinale*) plant extract was used to engineer AgNPs and employed for the degradation of environmental pollutants, i.e., azo dyes. Hu et al. (2007) and Wang et al. (2009) deposited Pd NPs on silicon nanowires to degrade methylene blue and eosin Y, respectively, in the presence of sodium borohydride.

Nanoparticles can be synthesized using various methods such as sonochemical, photochemical production, solvothermal electrochemical reduction, microwave irradiation, laser-mediated technique, chemical precipitation, sol-gel method, and thermal decomposition (Bilal et al., 2017b; Rasheed et al., 2017; Sathiyavimal et al., 2018; Saratale et al., 2018). Though these synthesis routes are facile and provide high yields, the excessive use of harsh chemicals remains a major concern. Hence, alternative methods utilizing biological sources to fabricate NPs will provide a cost-effective, non-toxic, biocompatible and eco-friendly approach (Bilal et al., 2017c; Pugazhendhi et al., 2018, 2019). Moreover, the biological synthesis using plant extracts is preferred over other methods. Considering these points, plant-based synthesis is becoming a meaningful approach for obtaining eco-friendly metal and metal oxide NPs or quantum dots (Jacob et al., 2019). Literature survey revealed that a wide variety of plant extracts such as *Artocarpus heterophyllus*, *Annona squamosa*, bamboo charcoal, banana peel, *Euphorbia tirucalli*, *Convolvulus arvensis*, *Cinnamomum camphora*, *Capsicum annuum,* Eucalyptus hybrids, *Ruellia tuberose,* and *Emblica officinalis* have been used to synthesize metal oxide NPs with multipurpose functionalities (Rasheed et al., 2017; Vasantharaj et al., 2019a,b). *T. officinale*, also known as dandelion, is a flowering herbaceous perennial plant of the family *Asteraceae*. It is a well-known medicinal plant containing numerous polyphenolic compounds, categorized as flavonoids (chrysoeriol, luteolin, quercetin, and their glycosides) and phenolic acids (caffeic acid, caftaric acid, chlorogenic, coumaric, etc.) (Miłek et al., 2019). Dandelion has long been exploited as non-toxic medicinal herb owing to its anti-inflammatory, choleretic, and diuretic properties. In many countries, it grows in residential and recreational lawns, on roadsides, and shores of waterways (Saratale et al., 2017).

This paper reports on the fabrication of CoNPs using *T. officinale* plant extract. As developed CoNPs were designated as TO-CoNPs and characterized by UV–Vis spectroscopy, Fourier transform infrared spectroscopy (FT-IR), and X-ray diffraction (XRD), dynamic light scattering (DLS), scanning electron microscopy (SEM), and transmission electron microscopy (TEM). The optimally yielded and stable TO-CoNPs were employed for the reductive degradation of synthetic azo dyes.

2. Material and methods

2.1. Chemical, reagents, dyes, and plant extract

All chemicals/reagents used in this study were of analytical laboratory grade with overall purity (> 99%) and used as received. Briefly, cobalt sulfate ($CoSO_4$), tetrabutylammonium bromide (TBAB), potassium bromide (KBr), sodium borohydride ($NaBH_4$) and acetone were obtained from local representative suppliers of Sigma-Aldrich, USA. The test dyes, i.e., direct yellow-142 (DY-142) and methyl orange (MO) were obtained from Dynasty Chemical Co. Ltd. Ningbo, China. The physiochemical characteristics of the dyes used in this study are summarized in Table 1. Healthy *T. officinale* leaves were collected from the botanical garden, Shanghai Jiao Tong University, Shanghai, China.

2.2. Pre-processing/preparation of plant extract

Fresh *T. officinale* leaves were washed three to four times using warm water to remove the surface dirt to avoid potential contamination. Thoroughly washed leaves were first dried at room temperature (28 ± 2 °C) and then grounded to a fine powder by an electrical blender. As obtained powder was sieved to remove the unwanted plant debris particles. Airtight plastic (polyethylene) bags were used to store the freshly prepared *T. officinale* leaves powder and subsequently used for extract preparation. Briefly, 1-g *T. officinale* leaves powder was soaked for 30 min in 100 mL deionized water at 28 ± 2 °C and then subjected to the rotary evaporator at 60 ± 3 °C. At the end of the stipulated evaporation period, the concentrated liquid was subject to lyophilization to acquire pure extract and refrigerated at 4 °C and used for the fabrication of TO-CoNPs.

2.3. Fabrication of TO-CoNPs

The fabrication of TO-CoNPs was first optimized using various reaction parameters via the classical approach. Briefly, 1-g $CoSO_4$ was mixed in 50 mL deionized water and poured in the same quantity of *T. officinale* leaves extract in the presence of TBAB (as a stabilizer agent). The above mixture was then gently stirred at room temperature (28 ± 2 °C) for 30 min, and the aqueous solution was decanted off. To remove the excessive and unreacted chemicals, as received TO-CoNPs were washed first with water and then acetone. The collected TO-CoNPs were purified by centrifugation at 4000 × *g* for 15 min, washed with deionized water and dried under vacuum. The collected TO-CoNPs were used for further characterizations.

2.4. Characterization of TO-CoNPs

Various instrumental techniques including UV–Vis spectroscopy, Fourier transform infrared spectroscopy (FT-IR), scanning electron microscopy (SEM), and transmission electron microscopy (TEM) were employed for characterization of TO-CoNPs. For an initial and absorbance-based confirmation of TO-CoNPs formation, UV–Vis Spectroscopy was performed using a Shimadzu UV–visible spectrophotometer (UV-2600). Around, 300 µL of TO-CoNPs was poured into 1.0 cm path length quartz cell following by addition of 2 mL deionized water. The absorbance was recorded in the wavelength ranging from 280 to 800 nm. The FTIR Spectroscopy (100 FTIR PerkinElmer Spectrometer) was used to perform FTIR analysis in the range of 500–4000 cm^{-1} with a resolution setting of 4 cm^{-1}. The surface morphology was analyzed using SEM (JEOL-7401F) and TEM (TF30 JOEL 2100F) at an accelerating voltage of 1 kV or 5 kV. The samples (TO-CoNPs) were mounted onto the clean silicon chips followed by gold sputtering. The deposition current of 20 mA for 2.0 min was used under the operating pressure of 7×10^{-2} bar. High definition images (HDI) were recorded at different magnifications.

2.5. Dye degradation potential of TO-CoNPs

The catalytic dye reduction potential of newly engineered TO-CoNPs was tested against two synthetic dyes, i.e., direct yellow-142 (DY-142) and methyl orange (MO). Briefly, a 50 mL centrifuge tube was used as a reaction vessel under continuous stirring at 20 rpm and 28 ± 2 °C. The centrifuge tube was fixed on a rotator (20 rpm) to allow a homogenous dispersion of TO-CoNPs in the reaction solution to maintain the solution uniformity during the catalytic reduction reaction process. The reaction solution was comprised of 3.0 mg catalytic agent, i.e., TO-CoNPs, target dyes, i.e., DY-142 and MO each separately at the concentration of 100 mg/L and 30 mL deionized water. The time-dependent absorbances were continuously monitored via UV–Vis spectral analysis at respective dyes wavelengths. Additionally, the control reactions were also carried out in parallel in the absence of the catalytic agent, i.e., TO-CoNPs.

2.6. Statistical analysis

A triplicate (n = 3) sampling approach was used in all experiments. The presented results are the average data values of three parallel triplicates ± standard deviation (SD) values. The standard deviation in Figurative data is shown as Y-error bars.

3. Results and discussion

3.1. TO-CoNPs confirmation via UV–Vis Spectroscopy

The formation of the cobalt (III) oxide NPs was confirmed by the UV–Visible spectrometry (Fig. 1). The as-prepared cobalt (III) oxide NPs display an absorption maximum at 319 nm, which is characteristic absorption peak of Co (III) oxide NPs. This band owes its existence due to surface Plasmon resonance band (Ghorbani et al., 2015) and the broad peak representing the wide size distribution of these particles. CoNPs were synthesized from the reduction of cobalt(II) nitrate hexahydrate using *Punica granatum* peel extract, which acts as a capping, reducing, and stabilizing agent (Bibi et al., 2017). One-step green biosynthesis of cobalt NPs involves the nucleation and growth processes through reduction of cobalt ions into neutral cobalt atoms, and the particles are nucleated and stabilized with the bioactive phenolic compound in plant extracts (Lisiecki and Pileni, 2003). The presence of carboxylic and hydroxyl groups in phenolic compounds have a high affinity to combine with metals. On chelate formation, the hydrogen is removed from ortho position of phenolic hydroxyl group resulting in a semi-quinone type structure. H^{+} radical is generated owing to the electron losing property of ellagic acid. Consequently, Co(II) is reduced to Co atom and nano-sized particles are produced due to the capping effect of bioactive compounds (Kahrilas et al., 2013).

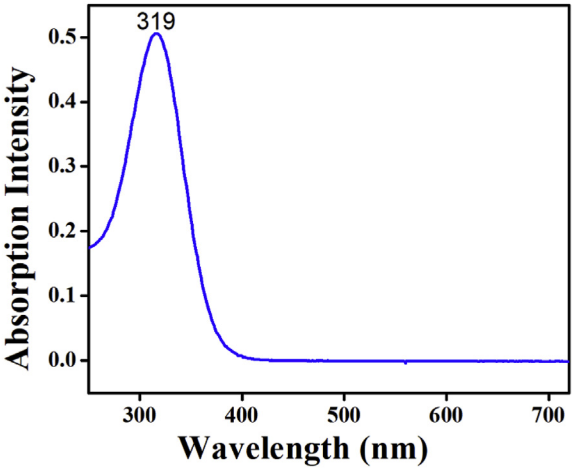

Fig. 1. UV–Visible spectrum of cobalt (III) oxide nanoparticles.

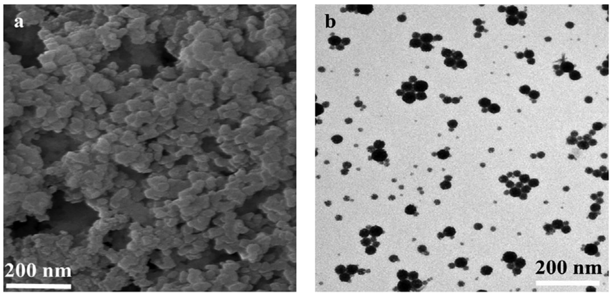

Fig. 2. (a) SEM and (b) TEM pictograph of cobalt (III) oxide nanoparticles.

3.2. Morphological characterization via SEM and TEM

The morphology of the CoNPs was investigated by SEM as shown in Fig. 2a. In the SEM image, the cobalt (III) oxide NPs were joined closely forming aggregates with variable distances. It is evident that the cobalt (III) oxide NPs were almost spherical with an average size of 50–100 nm. The cobalt (III) oxide NPs were further characterized by TEM as shown in Fig. 2b. It is clear from the TEM that these nanoparticles were spherical and most of the cobalt (III) oxide nanoparticles were physically joined but closely scattered with equal distances. Aggregation of the NPs primarily depend upon the nature of the plant extract and the phytochemicals since these biomolecules cap and stabilize the individual particle. The particles appear to be agglomerated due to intermolecular hydrogen bonding among these biological agents (Nazeruddin et al., 2014). In an earlier study, Bibi et al. (2017) synthesized uniform and spherical shape cobalt-oxide NPs using *P. granatum* peel extract agglomerated with an average size of less than 80 nm. Similarly, Vijayanandan and Balakrishnan (2018) also fabricated CoNPs using endophytic fungus and found to be spherical with good connectivity, dispersibility, and homogeneity between spheres. The aggregated NPs were adsorbed on the surface due to magnetic induction between the particles.

3.3. Fourier transform infrared spectroscopy (FT-IR)

The FTIR spectroscopy was used to study the surface chemistry of the obtained cobalt (III) oxide NPs. The FTIR spectrum is given in Fig. 3, which indicates the presence of several functional groups involved in the formation of cobalt (III) oxide NPs (Yedurkar et al., 2016). There are six noticeable absorption peaks in the FTIR spectrum at 3311, 2919, 172, 1580, 1433 and 1027 cm^{-1}. The extensive absorption peak at 3311 cm^{-1} attributes to the OH-stretching of hydroxyl groups or the presence of free OH groups. The absorption at 2919 and 1729 cm^{-1} are

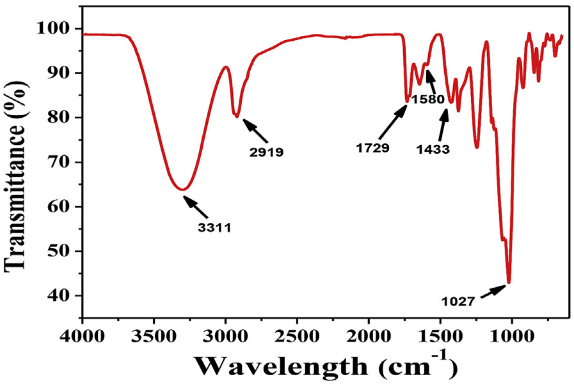

Fig. 3. FTIR spectrum of cobalt (III) oxide nanoparticles.

due to stretching vibration of C–H alkanes and –C═O- alkene groups respectively and played a vital role in the formation of green bio-synthesized cobalt (III) oxide NPs. The absorption bands at 1433 and 1027 cm^{-1} are due to stretching vibrations of C–N and C–O in amino acid (Yedurkar et al., 2016). The characteristic absorption bands of various functional groups (i.e., phenols, acids, protein, and polypeptides) indicated the bio-synthesis of cobalt (III) oxide NPs from the biological reduction of cell-free *T. officinale* extract. Also, the binding of polypeptides and proteins to NPs is reported through negatively charged carboxylate groups of free cysteine residues free amine groups (Gou et al., 2014). It is therefore realized that polypeptides and proteins were responsible for the reduction and stability of cobalt (III) oxide NPs and are the main bioactive molecules in the *T. officinale* extract.

3.4. TO-CoNPs-assisted degradation of methyl orange dye

A typical UV–Vis spectrogram obtained at the beginning (t = 0 h, as a control) and after that taken every 15 min and until at the end of the degradation process (t = 60 min). The recorded UV–Vis time-dependent scanning spectra of methyl orange dye degradation process in the absence and presence of TO-CoNPs is shown in Fig. 4. As evident from the UV–Vis spectra (Fig. 4A and B), two characteristics absorption bands, i.e., (1) in the UV range (280 nm), and (2) in the visible range (464 nm) were observed. The earlier UV band/peak range belongs to the azo-related structures and represents the chromophore part of the dye molecule. While the later band/peak appeared in the visible range (464 nm) corresponds to the red color of the dye solution and used to screen the dye degradation process. The intensity of both bands/peaks at UV range (280 nm), and the visible range (464 nm) was significantly reduced and finally eliminated 96.24% of MO dye after the treatment with TO-CoNPs for 60 min. The disappearance of these dye structure-related peak confirms the destruction and/or degradation of chromophore components of MO dye. The disappearance of highlighted both peaks could be due to the cleavage of azo bonds (–N═N–) of completely conjugated chromophores in MO dye molecule. The $NaBH_4$ possesses a dual function, i.e., acts as an electron donor and hydrogen suppliers (Edison et al., 2016). It also changes the pH of the solution during the dye reduction process (Dong et al., 2014). As a result, the surface charge of CoNPs turned into positive, which in turn absorb dyes and BH_4^- concurrently on the surface of CoNPs. The catalytic reduction is then initiated by transmitting electrons from the donor BH_4^- to dyes, where the CoNPs accept electrons from BH_4^- ions and delivers towards the dye molecule (Vidhu and Philip, 2014). In this way, a large amount of hydrogen released by $NaBH_4$ can result in the degradation of dye molecules. A similar phenomenon of biocatalytic azo bond cleavage-based MO degradation has been reported in earlier studies, though using different biological degradation strategies using NPS or enzymes (Hailei et al., 2009; Bilal et al., 2017d; Rasheed et al., 2018).

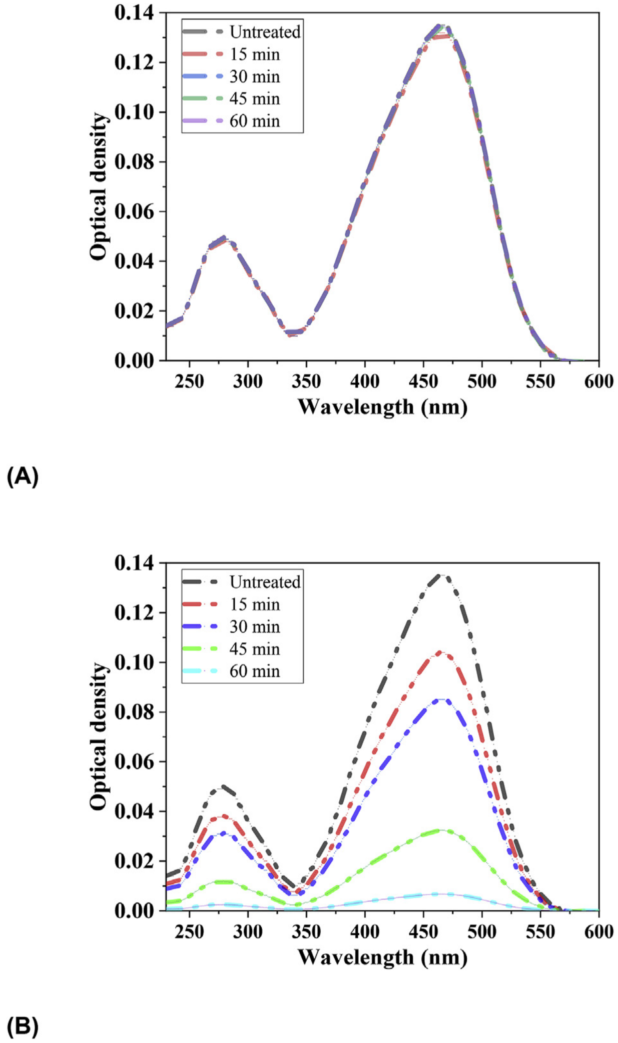

Fig. 4. A) Time-dependent UV–vis spectra of methyl orange dye in the absence of TO-CoNPs; **B)** Time-dependent UV–vis spectra of methyl orange dye in the presence of TO-CoNPs. (For interpretation of the references to color in this figure legend, the reader is referred to the Web version of this article.)

3.5. TO-CoNPs -assisted degradation of direct yellow-142 dye

Fig. 5 portrays the TO-CoNPs-assisted degradation profile of direct yellow-142 dye. The reduction-based removal of direct yellow-142 dye was subject to the reducing agent $NaBH_4$-assisted stable TO-CoNPs as a catalyst. The characteristic peak at 410 nm region was recorded during a time-dependent UV–Vis scanning of direct yellow-142 dye in the absence of TO-CoNPs (Fig. 5A). As evident from Fig. 5B, following TO-CoNPs-assisted treatment for 60 min, the peak intensity significantly reduced, and the dye decolorization of direct yellow-142 dye reached up to 93.37%. The azo functional group (R–N═N–R) of the dye was reduced to colorless amines (–NH–NH–) in the presence of a catalyst, i.e., $NaBH_4$-assisted stable TO-CoNPs. Recently, Rasheed et al. (2018) reported the catalytic potential of bio-synthesized silver NPs using *Convolvulus arvensis* extract for the degradation of environmental pollutants including a direct yellow-142 dye. As developed *C. arvensis* silver NPs were able to reduce azo dyes in the presence of $NaBH_4$ as a reducing agent. Finally, the reducing activity was evaluated the following the reduction in the optical density using UV–Vis spectrophotometer. Likewise, Edison et al. (2016) also reported the silver NPs (size range 20–50 nm) mediated reduction of direct yellow-12 dye in the presence of $NaBH_4$ as a reducing agent.

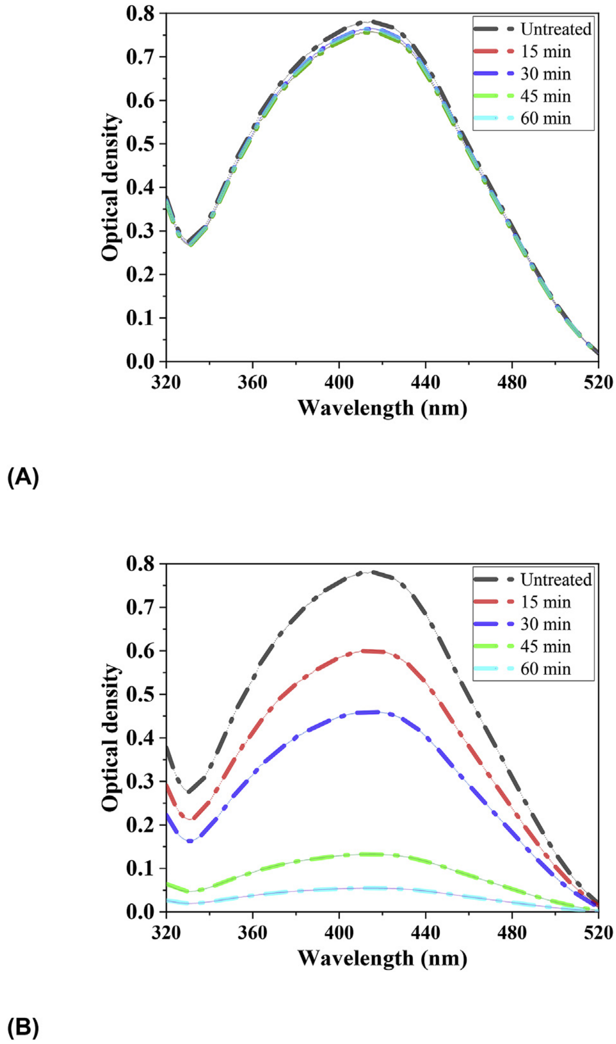

Fig. 5. A) Time-dependent UV–vis spectra of direct yellow- 142 dye in the absence of TO-CoNPs; **B)** Time-dependent UV–vis spectra of direct yellow 142 dye in the presence of TO-CoNPs. (For interpretation of the references to color in this figure legend, the reader is referred to the Web version of this article.)

4. Concluding remarks

Green and eco-friendly synthesis of TO-CoNPs was reported using naturally available *T. officinale* plant extract as a potential source. The characterization profile revealed that the naturally occurring phytoconstituents such as polyphenols in the *T. officinale* plant extract exhibited as capping agents during TO-CoNPs formation process, which additionally provide stability too. The morphological evaluation via SEM and TEM revealed the average size of 50–100 nm with spherical in shape. As developed TO-CoNPs catalyzed up to 96.24% and 93.37% degradation of methyl orange and direct yellow 142 dye, respectively, within 60 min using the $NaBH_4$ aqueous solution as a reducing agent. In summary, the results suggest that the newly developed TO-CoNPs could be a potential candidate to degrade toxic azo dyes. The highly efficient degradation of both dyes also enforces that TO-CoNPs may also be exploited for other related and emerging contaminants in a sophisticated manner.

Conflicts of interest

Authors have no conflict of interest in any capacity including competing and financial.

References

Bibi, I., Nazar, N., Iqbal, M., Kamal, S., Nawaz, H., Nouren, S., et al., 2017. Green and eco-friendly synthesis of cobalt-oxide nanoparticle: characterization and photo-catalytic activity. Adv. Powder Technol. 28 (9), 2035–2043.

Bilal, M., Adeel, M., Rasheed, T., Zhao, Y., Iqbal, H.M., 2019b. Emerging contaminants of high concern and their enzyme-assisted biodegradation–A review. Environ. Int. 124, 336–353.

Bilal, M., Asgher, M., Parra-Saldivar, R., Hu, H., Wang, W., Zhang, X., Iqbal, H.M., 2017a. Immobilized ligninolytic enzymes: an innovative and environmental responsive technology to tackle dye-based industrial pollutants–a review. Sci. Total Environ. 576, 646–659.

Bilal, M., Rasheed, T., Iqbal, H.M., Hu, H., Wang, W., Zhang, X., 2017b. Macromolecular agents with antimicrobial potentialities: a drive to combat antimicrobial resistance. Int. J. Biol. Macromol. 103, 554–574.

Bilal, M., Rasheed, T., Iqbal, H.M., Li, C., Hu, H., Zhang, X., 2017c. Development of silver nanoparticles loaded chitosan-alginate constructs with biomedical potentialities. Int. J. Biol. Macromol. 105, 393–400.

Bilal, M., Rasheed, T., Iqbal, H.M., Yan, Y., 2018a. Peroxidases-assisted removal of environmentally-related hazardous pollutants with reference to the reaction mechanisms of industrial dyes. Sci. Total Environ. 644, 1–13.

Bilal, M., Rasheed, T., Iqbal, H.M., Hu, H., Wang, W., Zhang, X., 2017d. Novel characteristics of horseradish peroxidase immobilized onto the polyvinyl alcohol-alginate beads and its methyl orange degradation potential. Int. J. Biol. Macromol. 105, 328–335.

Bilal, M., Rasheed, T., Nabeel, F., Iqbal, H.M., Zhao, Y., 2019a. Hazardous contaminants in the environment and their laccase-assisted degradation–A review. J. Environ. Manag. 234, 253–264.

Bilal, M., Rasheed, T., Sosa-Hernández, J., Raza, A., Nabeel, F., Iqbal, H., 2018b. Biosorption: an interplay between marine algae and potentially toxic elements—a review. Mar. Drugs 16 (2), 65.

Bokare, A.D., Chikate, R.C., Rode, C.V., Paknikar, K.M., 2008. Iron-nickel bimetallic nanoparticles for reductive degradation of azo dye Orange G in aqueous solution. Appl. Catal. B Environ. 79 (3), 270–278.

Dong, Z., Le, X., Liu, Y., Dong, C., Ma, J., 2014. Metal organic framework derived magnetic porous carbon composite supported gold and palladium nanoparticles as highly efficient and recyclable catalysts for reduction of 4-nitrophenol and hydrodechlorination of 4-chlorophenol. J. Mater. Chem. 2 (44), 18775–18785.

Edison, T.N.J.I., Lee, Y.R., Sethuraman, M.G., 2016. Green synthesis of silver nanoparticles using *Terminalia cuneata* and its catalytic action in reduction of direct yellow-12 dye. Spectrochim. Acta Mol. Biomol. Spectrosc. 161, 122–129.

Fathima, J.B., Pugazhendhi, A., Venis, R., 2017. Synthesis and characterization of ZrO_2 nanoparticles-antimicrobial activity and their prospective role in dental care. Microb. Pathog. 110, 245–251.

Fathima, J.B., Pugazhendhi, A., Oves, M., Venis, R., 2018. Synthesis of eco-friendly copper nanoparticles for augmentation of catalytic degradation of organic dyes. J. Mol. Liq. 260, 1–8.

Ghorbani, H.R., Mehr, F.P., Poor, A.K., 2015. Extracellular synthesis of copper nanoparticles using culture supernatants of *Salmonella typhimurium*. Orient. J. Chem. 31 (1), 527–529.

Gou, Y., Zhang, F., Zhu, X., Li, X., 2014. Biosynthesis and characterisation of silver nanoparticles using *Sphingomonas paucimobilis* sp. BDS1. IET Nanobiotechnol. 9 (2), 53–57.

Hailei, W., Ping, L., Min, P., Zhijun, Z., Guangli, Y., Guosheng, L., Jianming, Y., 2009. Rapid decolourization of azo dyes by a new isolated higher manganese peroxidase producer: *phanerochaete sp*. HSD. Biochem. Eng. J. 46 (3), 327–333.

Hu, H., Shao, M., Zhang, W., Lu, L., Wang, H., Wang, S., 2007. Synthesis of layer-deposited silicon nanowires, modification with Pd nanoparticles, and their excellent catalytic activity and stability in the reduction of methylene blue. J. Phys. Chem. C 111 (8), 3467–3470.

Jacob, J.M., Rajan, R., Aji, M., Kurup, G.G., Pugazhendhi, A., 2019. Bio-inspired ZnS quantum dots as efficient photo catalysts for the degradation of methylene blue in aqueous phase. Ceram. Int. 45 (4), 4857–4862.

Kahrilas, G.A., Wally, L.M., Fredrick, S.J., Hiskey, M., Prieto, A.L., Owens, J.E., 2013. Microwave-assisted green synthesis of silver nanoparticles using orange peel extract. ACS Sustain. Chem. Eng. 2 (3), 367–376.

Kusic, H., Koprivanac, N., Srsan, L., 2006. Azo dye degradation using Fenton type processes assisted by UV irradiation: a kinetic study. J. Photochem. Photobiol. A Chem. 181 (2–3), 195–202.

Lisiecki, I., Pileni, M.P., 2003. Synthesis of well-defined and low size distribution cobalt nanocrystals: the limited influence of reverse micelles. Langmuir 19 (22), 9486–9489.

Liu, L., Bilal, M., Duan, X., Iqbal, H.M., 2019. Mitigation of environmental pollution by genetically engineered bacteria—current challenges and future perspectives. Sci. Total Environ. 667, 444–454.

Miłek, M., Marcinčáková, D., Legáth, J., 2019. Polyphenols content, antioxidant activity, and cytotoxicity assessment of *Taraxacum officinale* extracts prepared through the micelle-mediated extraction method. Molecules 24 (6), 1025.

Naz, S., Khaskheli, A.R., Aljabour, A., Kara, H., Talpur, F.N., Sherazi, S.T.H., et al., 2014. Synthesis of highly stable cobalt nanomaterial using gallic acid and its application in catalysis. Advances in Chemistry 2014, Article ID 686925, 6 pages. https://doi.org/10.1155/2014/686925.

Nazeruddin, G.M., Prasad, N.R., Prasad, S.R., Garadkar, K.M., Nayak, A.K., 2014. In-vitro bio-fabrication of silver nanoparticle using *Adhathoda vasica* leaf extract and its antimicrobial activity. Phys. E Low-dimens. Syst. Nanostruct. 61, 56–61.

Pugazhendhi, A., Kumar, S.S., Manikandan, M., Saravanan, M., 2018. Photocatalytic properties and antimicrobial efficacy of Fe doped CuO nanoparticles against the pathogenic bacteria and fungi. Microb. Pathog. 122, 84–89.

Pugazhendhi, A., Prabhu, R., Muruganantham, K., Shanmuganathan, R., Natarajan, S., 2019. Anticancer, antimicrobial and photocatalytic activities of green synthesized magnesium oxide nanoparticles (MgONPs) using aqueous extract of *Sargassum wightii*. J. Photochem. Photobiol. B Biol. 190, 86–97.

Rasheed, T., Bilal, M., Li, C., Nabeel, F., Khalid, M., Iqbal, H.M., 2018. Catalytic potential of bio-synthesized silver nanoparticles using *Convolvulus arvensis* extract for the degradation of environmental pollutants. J. Photochem. Photobiol. B Biol. 181, 44–52.

Rasheed, T., Bilal, M., Li, C., Iqbal, H., 2017. Biomedical potentialities of *Taraxacum officinale*-based nanoparticles biosynthesized using methanolic leaf extract. Curr. Pharmaceut. Biotechnol. 18 (14), 1116–1123.

Rasheed, T., Bilal, M., Nabeel, F., Adeel, M., Iqbal, H.M., 2019. Environmentally-related contaminants of high concern: potential sources and analytical modalities for detection, quantification, and treatment. Environ. Int. 122, 52–66.

Saratale, R.G., Benelli, G., Kumar, G., Kim, D.S., Saratale, G.D., 2017. Bio-fabrication of silver nanoparticles using the leaf extract of an ancient herbal medicine, dandelion (*Taraxacum officinale*), evaluation of their antioxidant, anticancer potential, and antimicrobial activity against phytopathogens. Environ. Sci. Pollut. Control Ser. 25 (11), 10392–10406.

Saratale, R.G., Ghodake, G.S., Shinde, S.K., Cho, S.K., Saratale, G.D., Pugazhendhi, A., Bharagava, R.N., 2018. Photocatalytic activity of CuO/Cu (OH) 2 nanostructures in the degradation of Reactive Green 19A and textile effluent, phytotoxicity studies and their biogenic properties (antibacterial and anticancer). J. Environ. Manag. 223, 1086–1097.

Sathiyavimal, S., Vasantharaj, S., Bharathi, D., Saravanan, M., Manikandan, E., Kumar, S.S., Pugazhendhi, A., 2018. Biogenesis of copper oxide nanoparticles (CuONPs) using *Sida acuta* and their incorporation over cotton fabrics to prevent the pathogenicity of Gram negative and Gram-positive bacteria. J. Photochem. Photobiol. B Biol. 188, 126–134.

Sha, Y., Mathew, I., Cui, Q., Clay, M., Gao, F., Zhang, X.J., Gu, Z., 2016. Rapid degradation of azo dye methyl orange using hollow cobalt nanoparticles. Chemosphere 144, 1530–1535.

Vasantharaj, S., Sathiyavimal, S., Saravanan, M., Senthilkumar, P., Gnanasekaran, K., Shanmugavel, M., et al., 2019a. Synthesis of eco-friendly copper oxide nanoparticles for fabrication over textile fabrics: characterization of antibacterial activity and dye degradation potential. J. Photochem. Photobiol. B Biol. 191, 143–149.

Vasantharaj, S., Sathiyavimal, S., Senthilkumar, P., LewisOscar, F., Pugazhendhi, A., 2019b. Biosynthesis of iron oxide nanoparticles using leaf extract of *Ruellia tuberosa*: antimicrobial properties and their applications in photocatalytic degradation. J. Photochem. Photobiol. B Biol. 192, 74–82.

Vidhu, V.K., Philip, D., 2014. Catalytic degradation of organic dyes using biosynthesized silver nanoparticles. Micron 56, 54–62.

Vijayanandan, A.S., Balakrishnan, R.M., 2018. Biosynthesis of cobalt oxide nanoparticles using endophytic fungus *Aspergillus nidulans*. J. Environ. Manag. 218, 442–450.

Wang, F., Shao, M., Cheng, L., Chen, D., Fu, Y., Ma, D.D.D., 2009. Si/Pd nanostructure with high catalytic activity in degradation of eosin Y. Mater. Res. Bull. 44 (1), 126–129.

Yedurkar, S., Maurya, C., Mahanwar, P., 2016. Biosynthesis of zinc oxide nanoparticles using *Ixora coccinea* leaf extract—a green approach. Open J. Synth. Theor. Appl. 5 (01), 1.